Proton Spin–Lattice and Spin–Spin Relaxation Times in Isotactic Polypropylene. I. Effects of Crystallinity and Atactic Fraction*

HIROSHI TANAKA, *Macromolecular Research Laboratory, Faculty of Engineering, Yamagata University, Yonezawa, Yamagata, 992, Japan*

Synopsis

Spin–lattice relaxation time T_1 and spin–spin relaxation time T_2 were measured at 40°C on the isotactic polypropylene films of varying preparations and thermal history. T_1 increases with increasing crystallinity and two T_1's appear for the samples annealed at elevated temperatures (>120°C). These variations in T_1 are well interpreted in terms of the spin diffusion and decoupling of the mobile protons with immobile ones. A free induction decay following a 90° pulse is the superposition of three different decay curves, one of which is exponential and other two are nonexponential. There is an increase in T_{2a} with increasing crystallinity, which is indicative of the enhancement of the chain mobility in the amorphous region. There are differences between the crystallinity calculated from density and the fraction of crystalline region, F_c, obtained by the NMR method, which can be explained by the existence of the microparacrystals and the stress imposed on the amorphous chains on rapid cooling. On the other hand, there is a gradual lowering in T_1 and a considerable increase in T_{2a} as an atactic fraction is increased. The increase in atactic fraction also results in a decrease in the amount of the isotactic amorphous chains in the amorphous region.

INTRODUCTION

Nuclear magnetic resonance (NMR) has been extensively used for the study of solid polymers.[1] As for polypropylene, a number of workers have investigated the molecular motion of the polymer for a wide temperature range[2–19] by the measurements of second moment,[2–4,6,9–11,13,15,16] line width,[2,4–6,9–11,15,18] line shape,[3,13,15,18] T_1,[7,8,12–14,16,17,19] T_2,[7,13,17,19] and $T_{1\rho}$.[17,19] A line shape for oriented fibers at room temperature was also reported.[20] Furthermore, a line shape for the hard elastic polypropylene fibers has been studied in recent papers.[21–24] Most of these studies were carried out by a so-called CW method,[2–6,9–11,13,15,18,20–24] and only a few papers used pulse techniques,[7,8,12,14,16,17,19] the application of which has been significantly developed in recent years.

On the other hand, these investigations include the results with isotactic,[2–13,15–19,20–24] atactic,[2–6,8,10,14,15] and syndiotactic[15] polypropylene. In all these experiments a thermal history of the samples, however, is not necessarily clear, and the effects of annealing on a second moment, line width, and line shape are discussed only in a few papers.[4–6,20] In the present study the effects of thermal history and atactic fraction on the magnetic relaxation times of isotactic polypropylene were systematically investigated. It is well established that the mo-

* Presented in part at the 42nd Annual Meeting of the Japan Chemical Society, Osaka, April 1980.

Journal of Applied Polymer Science, Vol. 27, 2197–2208 (1982)
 CCC 0021-8995/82/062197-11$02.10

lecular motion is responsible for the relaxation times and closely relates to the physical structure of the polymer.[1] Because of instrumental limitations in our laboratory at present, relaxation times were only measured at 40°C. Nevertheless, it is believed that the data obtained can provide useful information about the physical structure of the polymer.

EXPERIMENTAL

Materials

The characteristics of the sample films used in this study are summarized in Table I.

TABLE I
Characteristics of Sample Films Used

Sample no.	$\overline{M}_v$[a]	Tacticity (%)[b]
1	265,000	94.4
2	295,000	92.4
3	302,000	89.4
4	281,000	85.2
5	265,000	81.0
6	233,000	66.2

[a] Measured in decalin solution at 135°C.
[b] Determined by extraction with boiling *n*-heptane.

Preparation of the Sample

Four series of the sample were prepared by varying the cooling conditions from the melt and the annealing conditions, the details of which are described below.

Series 1: A sample film (sample 1) was melt pressed at 230°C for 5 min between thin chrome-coated plates of 0.5 mm thickness and cooled in water of various temperatures. The temperatures varied were 0°C (ice water), 20°C, 40°C, 60°C, 80°C, and 100°C (boiling water). After immersion of 5 min in water of a desired temperature the sample was quenched in ice water.

Series 2: A melt-quenched sample, a sample which was melt-pressed at 230°C for 5 min and then quenched in ice water in series 1, was annealed in a poly(ethylene glycol)(PEG) bath at various temperatures for 1 h. After annealing, the sample was quenched in ice water. The temperatures employed were 80°C, 100°C, 120°C, 140°C, 150°C, and 155°C.

Series 3: Sample films (samples 2–6) were melt-pressed at 230°C for 5 min and quenched in ice water.

Series 4: Samples in series 3 were annealed at 155°C for 1 h in PEG and then quenched in ice water.

NMR Measurements

Spin–lattice and spin–spin relaxation times, T_1 and T_2, respectively, were measured using a Bruker P 20 wide line pulse spectrometer operating at a fixed frequency of 19.8 MHz at 40°C. The width of a 90° pulse was about 3 μs and

a recovery time was about 8.5 μs. T_1 measurements were carried out using a pulse sequence of 180°–t–90°. The values of T_2 and ratio of the rigid, intermediate, and mobile fractions in a sample, F_c, F_m, and F_a, respectively, were obtained from the free induction decay (FID) which follows a 90° pulse using the method reported by Fujimoto, Nishi, and Kado.[25] The signals obtained were accumulated on a Transient Memory M-100 E and Averager TMC-600 of Kawasaki Electronica Co., Ltd., to improve the S/N ratio. All the samples were cut in a shape of slender strip and packed in a sample tube.

Density Measurements and Calculation of Crystallinity

Densities of the samples were measured in a density gradient column prepared by mixture of water and n-propyl alcohol at 23°C. The crystallinity from the density was calculated from a two-phase model with the crystal density of 0.936 g/cm^3 [26] and the amorphous density of 0.858 g/cm^3.[27] On the other hand, the crystallinity from the NMR measurements, F_c, was obtained from the analysis of the FID.[25] Unless specifically noted, the crystallinity refers to that obtained from the density in the following section.

RESULTS AND DISCUSSION

Effects of Thermal History

In order to investigate the effects of crystallinity of the samples on the spin–lattice (T_1) and spin–spin relaxation times (T_2), a number of the samples with different crystallinities were prepared by varying the cooling conditions from the melt and the annealing conditions. In Table II are listed the data of crystallinity for the various samples prepared by different conditions.

It is well known from BPP theory[28] that T_1 has its minimum in the plot of T_1 vs. temperature at a temperature where $\omega_0\tau_c \fallingdotseq 1$ for each internal motion of the materials. Here, ω_0 and τ_c refer to the resonance frequency and the correlation time of internal motion. As for isotactic polypropylene, two T_1 minima have

TABLE II
Crystallinity for Samples Prepared at Different Conditions

Series	Sample preparing conditions		Crystallinity (%)
1	Cooling temp (°C)	0	39.2
		20	43.9
		40	49.3
		60	54.5
		80	58.2
		100	60.2
2	Annealing temp (°C) (annealing time = 1 h)	80	46.9
		100	53.4
		120	58.8
		140	64.0
		150	67.9
		155	71.3

been observed in all experiments.[8,12,13,16,17] The minimum located at a relatively low temperature (−120–−130°C) was assigned to the reorientation of methyl group,[8,12,13] and that which appears at a higher temperature (80–100°C) to the segmental motion of the polymer.[8,12,13] Although these temperatures which produce the T_1 minimum are dependent on the frequency used for the NMR measurement,[16] it is evident from the comparison of the frequency (21.5 MHz) used by Powles and Mansfield[12] with that of 19.8 MHz used in this experiment that the temperature of 40°C, which was employed in this experiment, is located at a lower temperature side of the T_1 minimum of the segmental motion.

In discussing the observed results, it was assumed that an isolated dipole pair reorients randomly with a single correlation time and the spin diffusion is operative when the protons of the immobile fraction are coupling with the mobile ones.[29–31] In fact, Crist and Peterlin have shown that the spin–lattice relaxation times of the entire sample can be explained by motion of a relatively small fraction of chain segments.[31–33] Furthermore, in this paper qualitative trends of change in T_1 values for the samples of various crystallinities are discussed without paying too much attention to absolute values which are affected by the impurities and paramagnetic substances.[28,29]

In Figures 1–3 are shown the data for the samples of series 1 (●) and series 2 (○). Figure 1 shows the effect of the increased crystallinity on T_1. As is shown in this figure, there is a monotonic increase in T_1 with increasing crystallinity of the samples cooled at different temperatures (●). There is general agreement that the constraints to the segmental motion in the amorphous region imposed by the presence of the crystallites elevate the temperature at which the motional

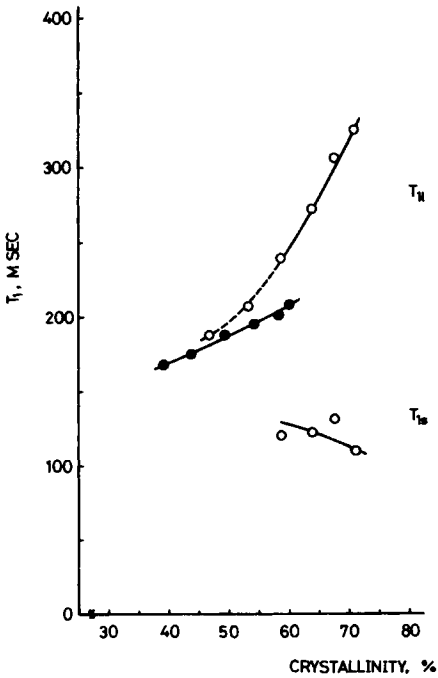

Fig. 1. A plot of T_1 as a function of crystallinity. T_{1l} and T_{1s} refer to a long T_1 and a short T_1, respectively. (●) Samples cooled from the melt at various cooling conditions (series 1); (○) samples annealed at various temperatures in PEG for 1 h (series 2).

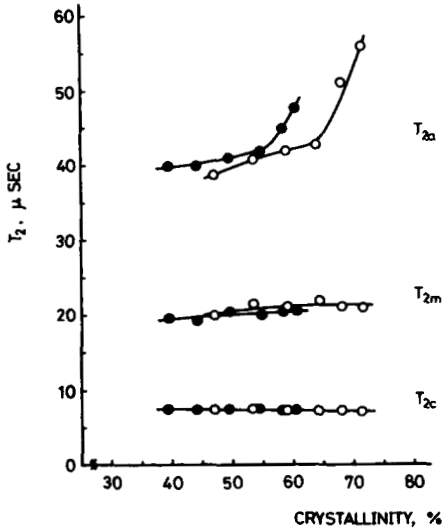

Fig. 2. Dependence of T_2 on crystallinity. T_{2a}, T_{2m}, and T_{2c} refer to T_2 of amorphous, intermediate, and crystalline regions, respectively. (●) Samples of series 1; (○) samples of series 2.

narrowing in the line shape and the rapid reduction of the second moment occur.[2-4,6,13] Similarly, the T_1 minimum for the segmental motion shifts to higher temperatures, owing to the presence of the crystallites.[8] Apart from this effect, the value of the T_1 minimum becomes shorter as the noncrystalline mass fraction is increased.[8,31-33] Thus, morphological changes introduced by the

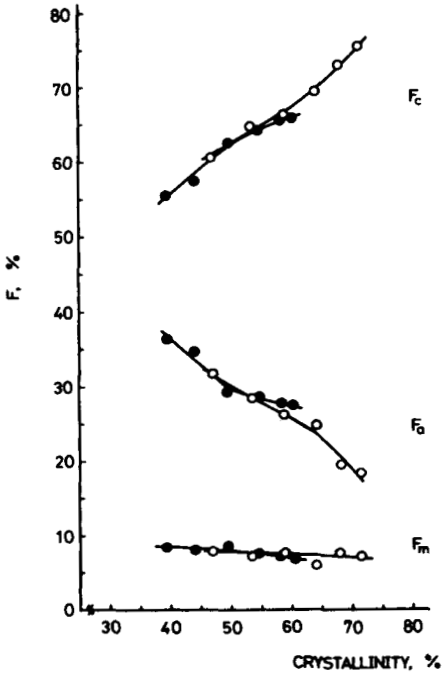

Fig. 3. Fractions of amorphous (F_a), intermediate (F_m), and crystalline (F_c) regions against crystallinity. (●) Samples of series 1; (○) samples of series 2.

various thermal treatments into the samples produce a change in T_1 value when measured at a constant temperature (at 40°C in this experiment); constraints to the segmental motion give rise to a higher value of T_1, and increase in crystallinity also results in a higher value of T_1.

It is well known from the Kubo–Tomita theory[34] that the FID curve is exponential and the signal decays as $\exp(-t/T_2)$ for nuclei spins with short τ_c as in a liquidlike amorphous region and the curve is nonexponential for those with long τ_c as in a rigid crystalline region and the signal decays as $\exp[-\frac{1}{2}(t/T_2)^2]$.

In a solid isotactic polypropylene, the FID measured at 40°C is nonexponential and the recorded traces are the superposition of three decay curves, one of which decays as $\exp(-t/T_2)$ and other two as $\exp[-\frac{1}{2}(t/T_2)^2]$. Three different relaxation times, T_{2a}, T_{2m}, and T_{2c} are obtained from these different decay curves. The longest relaxation time, T_{2a}, obtained from the curve which decays as $\exp(-t/T_2)$ can be attributed to the mobile (amorphous) region[29] and the shortest one, T_{2c}, to the rigid (crystalline) region.[35] T_{2m}, the value of which lies between T_{2a} and T_{2c}, is believed to associate with the intermediate region.[25] T_{2m} and T_{2c} are obtained from the curves which decay as $\exp[-\frac{1}{2}(t/T_2)^2]$.

T_2 is plotted as a function of the crystallinity in Figure 2. It has already been shown that T_{2a} becomes longer with increasing temperature,[17] which is indicative of the enhancement of the chain mobility in the amorphous region. Consequently, the fact that the increase in T_{2a} with increasing crystallinity for the samples of series 1 (●) indicates that there is a slight increase in the chain mobility in the amorphous region. On the contrary, F_a decreases gradually with increasing crystallinity, as shown in Figure 3.

Taking into account the increase in T_{2a} and decrease in F_a, it can be concluded that for the samples of series 1 the decrease in the amount of the amorphous region results in the increase in T_1. The fact that only one T_1 is obtained for these samples consisting of both crystalline and amorphous regions can be explained in terms of spin diffusion.[29–31]

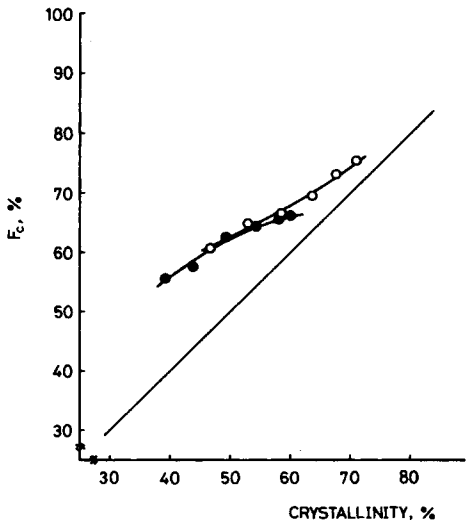

Fig. 4. A plot of F_c against crystallinity calculated from density. (●) Samples of series 1; (○) samples of series 2.

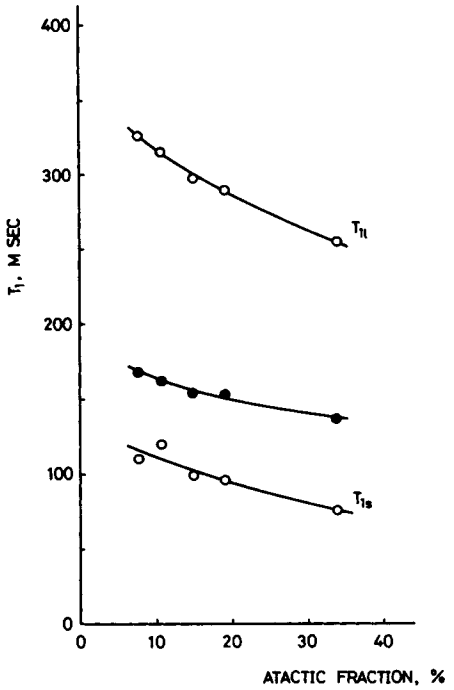

Fig. 5. A plot of T_1 as a function of atactic fraction. T_{1l} and T_{1s} refer to a long T_1 and a short T_1, respectively. (●) Melt-quenched samples (series 3); (○) samples annealed at 155°C for 1 h in PEG (series 4).

The situation is slightly different in the samples annealed at various temperatures. In this case, two T_1's appear for the samples annealed at temperatures above 120°C. T_{1l} and T_{1s} in Figure 1 refer to a long T_1 and a short T_1, respectively. In this case too, there is a monotonic, rather sharp increase in T_{1l} as the crystallinity is increased. The change in T_{1s}, however, is rather uncertain; probably a slight decrease in T_{1s} with crystallinity seems to occur. The results similar to those obtained for the samples of series 1 are shown in Figure 2. There

TABLE III
Crystallinity of Samples with Different Atactic Fractions

Series	Sample preparing conditions	Atactic fraction (%)	Crystallinity (%)
3	Melt-quenched	92.4	38.8
		89.4	37.9
		85.2	37.7
		81.0	37.0
		66.2	33.4
4	Annealed at 155°C for 1 h in PEG	92.4	72.2
		89.4	72.2
		85.2	68.8
		81.0	67.3
		66.2	58.8

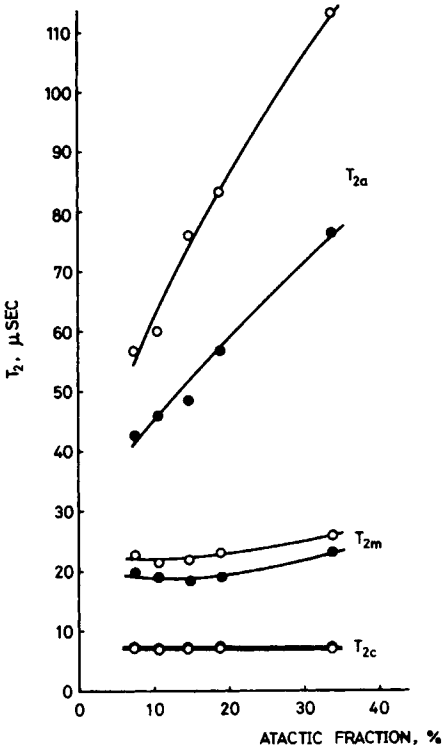

Fig. 6. Dependence of T_2 on atactic fraction. T_{2a}, T_{2m}, and T_{2c} refer to T_2 of amorphous, intermediate, and crystalline regions, respectively. (●) Melt-quenched samples (series 3); (○) annealed samples (series 4).

is a slight increase in T_{2a} for the lower crystallinity and a relatively sharp increase for the higher crystallinity. It is believed that the appearance of T_{1s} is closely related to a larger increase in T_{2a} in Figure 2, though T_{2a}'s of the samples annealed at 120°C (crystallinity = 58.8%) and 140°C (crystallinity = 64.0%) are not so long. The decrease in T_{1s} and increase in T_{2a} indicate the generation of the amorphous region which decouples with crystalline one.[31] The development of the decoupling between crystalline and amorphous regions and the enhancement of the chain mobility in the amorphous region which couples strongly to the lattice result in the faster spin–lattice relaxation, giving a smaller value of T_{1s}. The development of the decoupling is also reflected in an increase in T_{1l}, as shown in Figure 1. It must be noted that the different T_1 values can be obtained for the samples of the same crystallinity but with different thermal history.

There is no appreciable change in T_{2c} for all samples investigated and a slight increase in T_{2m} as the crystallinity is increased (Figure 2). As T_2 is measured from the FID, the dead time following a 90° pulse is of the same order of magnitude as T_{2c}. Therefore, a precise value for T_{2c} is not expected, and the main emphasis in this paper is on T_{2a} and T_1, which can provide useful information on the segmental motion in the amorphous region.

There is a relatively large increase in F_c and a decrease in F_a with increasing crystallinity, as shown in Figure 3. The amount of F_m, however, is almost unchanged for a wide range of crystallinity, but it cannot be decided only from this

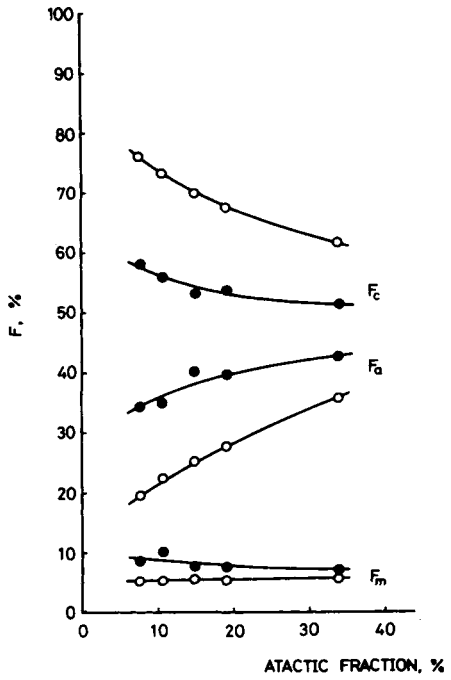

Fig. 7. Fractions of amorphous (F_a), intermediate (F_m), and crystalline (F_c) regions against atactic fraction. (●) Melt-quenched samples (series 3); (○) annealed samples (series 4).

figure that either the region corresponding to F_m is unchanged through the various thermal treatments or transformation from F_a to F_m and that from F_m to F_c mutually compensate, resulting in no substantial change in F_m. In addition, no explanation can be offered at present for the location of the chain segments which are included in F_m. This problem will be a subject of future study.

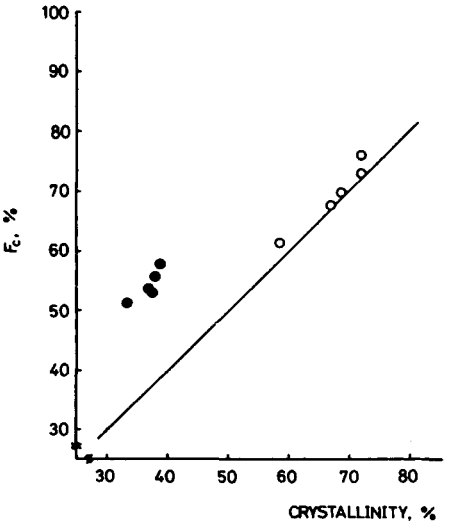

Fig. 8. A plot of F_c against crystallinity calculated from density. (●) Melt-quenched samples (series 3); (○) annealed samples (series 4).

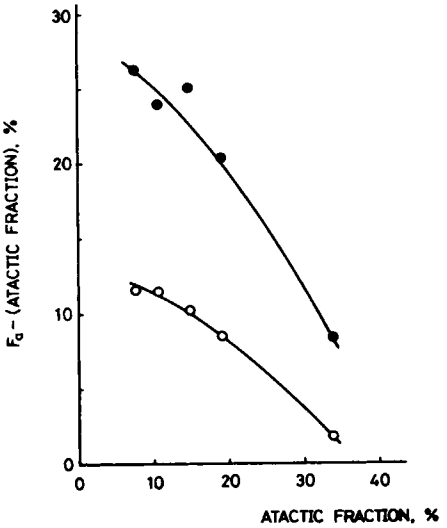

Fig. 9. A plot of isotactic amorphous fraction against atactic fraction. (●) Melt-quenched samples (series 3); (○) annealed samples (series 4).

Figure 4 shows the relation between the crystallinity calculated from the density and that obtained by NMR method, F_c. The solid circle represents the samples cooled at different temperatures (series 1), and the open circle represents those annealed at various temperatures (series 2). As the cooling and annealing temperatures are raised, the crystallinity of the samples increases, and F_c approaches the crystallinity calculated from the density, which indicates that the physical structure of the sample approaches the so-called two-phase model. It has already been shown by Miller[5] that the line width of narrow component at room temperature is slightly greater in the quenched sample than in the crystalline one, which is interpreted in terms of the constraints to motion on the amorphous region. Nishioka et al.[6] have also reported by the measurements of the line width that the volume of the constrained amorphous part would be larger in the quenched sample than in the annealed one. Taking these results into consideration, it is believed that the existence of the microparacrystal and the stress imposed on the amorphous region on rapid cooling are responsible for the disparity between the crystallinity calculated from the density and the fraction of crystalline region, F_c, obtained by the NMR method.

Influence of Atactic Fraction

In Figures 5–9 are shown the data for the samples with different atactic fractions. The crystallinity of the samples quenched from the melt (series 3) and annealed at 155°C for 1 h in PEG (series 4) are summarized in Table III.

Figure 5 shows the effect of increasing atactic fraction on T_1. Solid circles indicate the data with the melt-quenched samples, and open circles indicate those with the annealed ones. As is evident from this figure, all T_1 values decrease with increasing the amount of atactic fraction and annealing at 155°C results in some portions of the sample exhibiting a shorter T_1. As has already been shown, the T_1 minimum corresponding to the segmental motion is located at a

lower temperature for atactic polypropylene than for isotactic polypropylene, owing to the favorable chain mobility in the amorphous region.[8] The T_1 minimum also decreases with increasing noncrystalline mass fraction, as mentioned before.[8,31–33] The results shown in Figure 5 are in general agreement with the previous studies mentioned above.

In Figures 6 and 7 are plotted T_2 and F, respectively, as a function of atactic fraction for the melt-quenched and annealed samples. As is expected, F_a increases with increasing atactic fraction and T_{2a} increases also with atactic fraction, reflecting the higher mobility of the amorphous chains which have been restricted by the presence of the crystallites[3,4,6,13] composed of isotactic polypropylene. It is also expected that the increases in F_a and in T_{2a} lower the values of T_{1s}.[29] This expectation is already shown to be true in Figure 5. It is noteworthy that there is a very sharp increase in T_{2a} for the annealed samples as the atactic fraction is increased, indicating the significant enhancement of the chain mobility in the amorphous region. This change in chain mobility is accompanied by the morphological change which approaches more and more the physical structure of the sample two-phase model. To examine this trend more quantitatively, F_c is plotted as a function of crystallinity in Figure 8, similarly as in Figure 4. Solid and open circles refer to the melt-quenched (series 3) and annealed samples (series 4), respectively. The approach of the observed points to the solid line with annealing is thought to reflect the morphology which approaches more and more the two-phase model on annealing.

Generally, it is believed that the amorphous chains consist both of isotactic and atactic chains. In Figure 9 are plotted the amounts of isotactic amorphous chains as a function of the atactic fraction for the melt-quenched and annealed samples. There is a significant decrease in the isotactic amorphous chains with increasing atactic fraction. Furthermore, it is obvious that the annealing results in a considerable decrease in the amount of the isotactic amorphous chains. These features indicate that large portions of isotactic chains in the amorphous region crystallize on annealing and the amorphous region consists mainly of the atactic chains as the atactic fraction is increased.

The author wishes to thank Dr. K. Sato of Idemitsu Kosan Co., Ltd., and Dr. T. Nishi of Tokyo University for many helpful discussions. He also thanks the Chisso Corp. for supplying the samples with different atactic fractions.

References

1. V. J. McBrierty, *Polymer*, **15,** 503 (1974).
2. W. P. Slichter and E. R. Mandell, *J. Chem. Phys.*, **29,** 232 (1958).
3. J. A. Sauer, R. A. Wall, N. Fuschillo, and A. E. Woodward, *J. Appl. Phys.*, **29,** 1385 (1958).
4. W. P. Slichter and E. R. Mandell, *J. Appl. Phys.*, **29,** 1438 (1958).
5. R. L. Miller, *Polymer*, **1,** 135 (1960).
6. A. Nishioka, Y. Koike, M. Owaki, T. Naraba, and Y. Kato, *J. Phys. Soc. Jpn.*, **15,** 416 (1960).
7. A. Hirai and T. Kawai, *Mem. Coll. Sci. Univ. Kyoto, A*, **29,** 345 (1961).
8. T. Kawai, Y. Yoshimi, and A. Hirai, *J. Phys. Soc. Jpn.*, **16,** 2356 (1961).
9. A. E. Woodward, A. Odajima, and J. A. Sauer, *J. Phys. Chem.*, **65,** 1384 (1961).
10. R. P. Gupta, *Kolloid Z.*, **174,** 73 (1961).
11. R. P. Gupta, *Kolloid Z.*, **174,** 74 (1961).
12. J. G. Powles and P. Mansfield, *Polymer*, **3,** 339 (1962).
13. M. P. McDonald and I. M. Ward, *Proc. Phys. Soc.*, **80,** 1249 (1962).
14. W. P. Slichter, *J. Polym. Sci., C*, **14,** 33 (1966).

15. A. Chierico, G. Del Nero, G. Lanzi, and E. R. Mognaschi, *Eur. Polym. J.*, **2**, 339 (1966).
16. U. Kienzle, F. Noack, and J. von Schütz, *Kolloid Z.*, **236**, 129 (1970).
17. V. J. McBrierty, D. C. Douglass, and D. R. Falcone, *J. Chem. Soc. Faraday Trans. II*, **68**, 1051 (1972).
18. K. Bergmann, *Kolloid Z.*, **251**, 962 (1973).
19. V. J. McBrierty, D. C. Douglass, and P. J. Barham, *J. Polym. Sci., Polym. Phys. Ed.*, **18**, 1561 (1980).
20. D. Hyndman and G. F. Origlio, *J. Polym. Sci.*, **39**, 556 (1959).
21. H. Čačković, R. Hosemann, and J. Loboda-Čačković, *J. Polym. Sci., Polym. Lett. Ed.*, **16**, 129 (1978).
22. J. Loboda-Čačković, H. Čačković, and R. Hosemann, *Makromol. Chem.*, **180**, 291 (1979).
23. R. P. Wool, M. I. Lohse, and T. J. Rowland, *J. Polym. Sci., Polym. Lett. Ed.*, **17**, 385 (1979).
24. J. Loboda-Čačković, H. Čačković, and R. Hosemann, *J. Macromol. Sci. Phys., B*, **16**(1), 127 (1979).
25. K. Fujimoto, T. Nishi, and R. Kado, *Polym. J.*, **3**, 448 (1972).
26. G. Natta, P. Corradini, and M. Cesari, *Atti. Acad. Naz. Lincei Rend. Classe Sci. Fis. Mat. Nat.*, **21**, 365 (1956).
27. F. Danusso, G. Maraglio, W. Ghigla, L. Motte, and G. Talamini, *Chim. Ind.*, **XLI**, 748 (1959).
28. N. Bloembergen, E. M. Purcell, and R. V. Pound, *Phys. Rev.*, **73**, 679 (1948).
29. D. W. McCall and D. C. Douglass, *Polymer*, **4**, 433 (1963).
30. J. E. Anderson and W. P. Slichter, *J. Phys. Chem.*, **69**, 3099 (1965).
31. B. Crist and A. Peterlin, *J. Polym. Sci., A-2*, **7**, 1165 (1969).
32. B. Crist and A. Peterlin, *J. Macromol. Sci. Phys., B*, **4**, 791 (1970).
33. B. Crist and A. Peterlin, *J. Polym. Sci., A-2*, **9**, 557 (1971).
34. R. Kubo and K. Tomita, *Phys. Soc. Jpn.*, **9**, 888 (1954).
35. D. W. McCall, D. C. Douglass, and D. R. Falcone, *J. Phys. Chem.*, **71**, 998 (1967).

Received September 25, 1981
Accepted December 14, 1981